Single-Nucleotide-Specific siRNA Targeting in a Dominant-Negative Skin Model

Robyn P. Hickerson[1], Frances J.D. Smith[2], Robert E. Reeves[3], Christopher H. Contag[3,4], Devin Leake[5], Sancy A. Leachman[6], Leonard M. Milstone[7], W.H. Irwin McLean[2] and Roger L. Kaspar[1]

RNA interference offers a novel approach for developing therapeutics for dominant-negative genetic disorders. The ability to inhibit expression of the mutant allele without affecting wild-type gene expression could be a powerful new treatment option. Targeting the single-nucleotide keratin 6a (K6a) N171K mutation responsible for the rare monogenic skin disorder pachyonychia congenita (PC), we demonstrate that small interfering RNAs (siRNAs) can potently and selectively block expression of mutant K6a. To test whether lead siRNAs could discriminate mutant mRNA in the presence of both wild-type and mutant forms, a dominant-negative PC cell culture model was developed. As predicted for a dominant-negative disease, simultaneous expression of both wild-type and mutant K6a resulted in defective keratin filament formation. Addition of mutant-specific siRNAs allowed normal filament formation, suggesting selective inhibition of mutant K6a. The effectiveness of our siRNA in skin was tested by co-delivering a firefly luciferase/mutant K6a bicistronic reporter construct and mutant-specific siRNAs to mouse footpads. Potent inhibition of the fluorescent reporter was demonstrated using the Xenogen IVIS200 *in vivo* imaging system. Additionally, wild type-specific siRNAs knocked down the expression of pre-existing endogenous K6a in human keratinocytes. These results suggest that efficient delivery of these "designer siRNAs" may allow effective treatment of numerous genetic disorders including PC.

Journal of Investigative Dermatology (2008) **128,** 594–605; doi:10.1038/sj.jid.5701060; published online 11 October 2007

INTRODUCTION

In the decade and a half that has followed the initial discovery of the underlying keratin 5 (K5) and K14 gene mutations in epidermolysis bullosa simplex (EBS) (Bonifas *et al.*, 1991; Coulombe *et al.*, 1991; Lane *et al.*, 1992), there has been a plethora of additional research identifying the genetic basis of many epithelial fragility disorders with 20 of the 54 human keratin genes now linked to genetic diseases, including pachyonychia congenita (PC) (Irvine and McLean, 1999; McLean *et al.*, 2005; Smith *et al.*, 2005). Furthermore, mutations have now been identified in genes encoding many non-keratin intermediate filament proteins (Omary *et al.*, 2004). Collectively, these genetic disorders affect many non-epithelial organ systems, and include muscular dystrophies, neuropathies, inherited cataracts, progerias, and lipodystrophies; so keratinopathies are part of a large, clinically heterogeneous group of disorders that share a common dominant-negative pathomechanistic basis. Despite these significant discoveries, little progress has been made in developing therapeutics for these disorders or other dominantly inherited genetic diseases. The discovery of RNA interference (RNAi) and the demonstration that small interfering RNAs (siRNAs) can potently and specifically inhibit gene expression suggests that application of this technology may result in novel therapeutics for skin disorders (Lewin *et al.*, 2005; Hengge, 2006; Prud'homme *et al.*, 2006; Dykxhoorn *et al.*, 2006a). siRNA-based therapeutics are currently in clinical trials for a number of non-skin diseases, including age-related macular degeneration and respiratory syncytial virus (Dykxhoorn and Lieberman, 2006).

PC is a dominant-negative skin disorder resulting from mutations in any one of the inducible keratin genes produced by keratinocytes: K6a, K6b, K16, and K17 (Smith *et al.*, 2005; Leachman *et al.*, 2005). Keratins are type I and type II intermediate filament proteins that form a cytoskeletal network within all epithelial cells. Mutations in keratin genes result in aberrant cytoskeletal networks, which present clinically as a variety of epithelial fragility phenotypes such as PC (Smith, 2003). The majority of keratin mutations are heterozygous missense mutations; in some cases, small in-frame deletion/insertion mutations

[1]*TransDerm Inc., Santa Cruz, California, USA;* [2]*Human Genetics Unit, Ninewells Hospital and Medical School, University of Dundee, Dundee, UK;* [3]*Molecular Imaging Program at Stanford (MIPS), and Departments of Radiology, Microbiology and Immunology, Stanford University School of Medicine, Stanford, California, USA;* [4] *Departments of Pediatrics and Pathology, Stanford University School of Medicine, Stanford, California, USA;* [5]*Thermo Fisher Scientific, Dharmacon Products, Lafayette, Colorado, USA;* [6]*Department of Dermatology, University of Utah, Salt Lake City, Utah, USA and* [7]*Department of Dermatology, Yale University, New Haven, Connecticut, USA*

Correspondence: Roger L. Kaspar, 2161 Delaware Avenue, Suite D, Santa Cruz, California 95060, USA. E-mail: roger.kaspar@tansderminc.com

Abbreviations: EBS, epidermolysis bullosa simplex; EGFP, enhanced green fluorescent protein ; EYFP, enhanced yellow fluorescent protein; K, keratin; NSC4, non-specific control; PC, pachyonychia congenita; RNAi, RNA interference; siRNA, small interfering RNA; tdTFP, tomato fluorescent protein

Received 29 May 2007; revised 27 June 2007; accepted 1 July 2007; published online 11 October 2007

have been reported (see the Intermediate Filament Mutation database; http://www.interfil.org). Most mutations occur in the highly conserved helix boundary motif domains located at either end of the α-helical keratin rod domain. There are several recurrent mutations; the major one for K6a is at the N171 site, at which the codon is either deleted or a single base pair is mutated resulting in an amino-acid change (e.g. N171K). These helix boundary mutations presumably prevent normal intermediate filament formation (Steinert *et al.*, 1993) and compromise the structural integrity of the affected keratinocytes, as seen ultrastructurally in the epidermis of PC patients (McLean *et al.*, 1995), resulting in the various PC symptoms (Leachman *et al.*, 2005).

PC was chosen as a prototype disorder for development of siRNA-based therapeutics to treat genetic skin disorders as (1) the molecular basis and cell type have been identified, (2) the dominant-negative pattern potentially allows for downregulation of the mutant keratin resulting in a therapeutic effect if wild-type expression is unaffected, and (3) the major patient complaint is localized pain, usually at small, defined pressure points on the feet, suggesting that a small area can be locally treated (Leachman *et al.*, 2005; Smith *et al.*, 2006). In this study, the ability to design and identify potent siRNAs that can discriminate a single-nucleotide change in K6a was investigated.

RESULTS

Differential inhibition of mutant K6a *versus* wild type by specific siRNAs in tissue culture cells

A fluorescence-based tissue culture assay was developed to screen for siRNAs that block mutant K6a expression with little or no effect on wild-type expression. To readily monitor K6a expression, both mutant and wild-type forms of K6a were fused to the enhanced yellow fluorescent protein (EYFP) reporter gene (Figure 1a). All possible siRNAs (19 + 2 format, see Materials and Methods), designed to target the K6a mRNA region containing a single-nucleotide change (C→A at nucleotide position 513 resulting in the amino-acid change, N171K), were tested (Figure 1b). Mutant-specific siRNAs (K6a_513a.1–19) and wild-type-specific siRNAs (K6a_513c.1–19) will be referred to as MUT.1–19 and WT.1–19, respectively. siRNAs were co-transfected into 293FT cells with plasmids that express either K6a-WT/EYFP or K6a-N171K/EYFP (Figure 1c). As a positive control, enhanced green fluorescent protein (EGFP)-specific siRNAs were co-transfected with the mutant and wild-type K6a/EYFP constructs, resulting in 97 and 96% inhibition, respectively (the 50% inhibitory concentration (IC_{50}), values were 0.1 nM against both constructs). It should be noted that EYFP and EGFP are nearly identical in sequence, and there are no nucleotide differences in the site targeted by the EGFP siRNA. Several mutant-specific inhibitors showed activity against mutant expression; however, each showed significant activity against wild-type expression as well (i.e. MUT.2, 3, 5, 6, and 19). Other siRNAs were ineffective against either target (i.e. MUT.8, 9, and 13–17). MUT.4, 10, and 12 showed discrimination between mutant and wild-type K6a targets, with MUT.4 and MUT.12 exhibiting the greatest potency. MUT.4 reduced expression of mutant K6a by 88%, whereas wild-type expression was reduced only by 23% (IC_{50} values for MUT.4 against the mutant and wild-type constructs were 0.2 and >4 nM, respectively). MUT.12 reduced mutant K6a expression by 82%, whereas the wild-type construct was completely unaffected under the conditions tested (IC_{50} value for MUT.12 against the mutant K6a target was 0.3 nM). The data were corrected against cells transfected with the irrelevant *n*on-specific *c*ontrol (NSC4) siRNA, which did not inhibit K6a/EYFP expression (<5% variation, data not shown). It should be noted that no changes in cell morphology or cell density were observed by bright-field microscopy after siRNA treatment (data not shown).

The complete set of siRNAs that target the wild-type K6a sequence (''C'' nucleotide at mRNA position 513) was also tested. In general, the same inhibition pattern was observed (see Figure S1). WT.4 siRNA had no effect on mutant K6a expression, whereas wild-type expression was reduced by 65%. WT.12 inhibited wild-type expression by 80%, whereas mutant expression was reduced by 18%. To test further the requirement for an exact complementary match at position 513, additional siRNAs containing ''U'' or ''G'' residues at this site were tested (Figure 2a). For each of the two sets of siRNAs tested, only the exact match inhibited gene expression when co-transfected with the mutant or wild-type K6a/EYFP expression plasmid (Figure 2b and see Figure S2 for quantitative data). These results indicate that mutant-specific siRNAs can be designed that preferentially inhibit mutant K6a gene expression over wild type and vice versa (i.e. wild-type-specific siRNAs can selectively inhibit wild-type expression).

Preferential inhibition of mutant K6a results in normal keratin filament formation in a dominant-negative PC tissue culture model

The siRNAs shown to selectively target mutant K6a/EYFP over wild type were used to determine whether mutant-specific siRNAs can preferentially inhibit mutant K6a protein synthesis in PLC cells that have been transfected with a mixture of both mutant and wild-type K6a expression constructs (tissue culture model for the dominant-negative PC disorder). Human PLC hepatocytes were used in these experiments, as intermediate filaments are readily visualized in the cells following transfection of exogenous keratins owing to their flat morphology and simple keratin expression profile; PLC cells express mainly K8 and K18 (Woll *et al.*, 2005). The ability of the identified inhibitors to selectively block mutant K6a expression was assayed by analyzing the percentage of cells in which keratin filaments were normal or disorganized (aggregates). As seen in Figure 3, cells that were transfected with the wild-type K6a/EYFP construct preferentially formed keratin filaments, whereas cells transfected with the mutant K6a/EYFP construct contained keratin aggregates with little, if any, evidence of filament formation, as determined by detection of the EYFP tag by fluorescence microscopy (76 *vs* 3% of the cells contained predominantly filaments when transfected with the wild-type or mutant construct, respectively). As expected for a dominant-negative mechanism, cells transfected with a mixture of wild-type and mutant

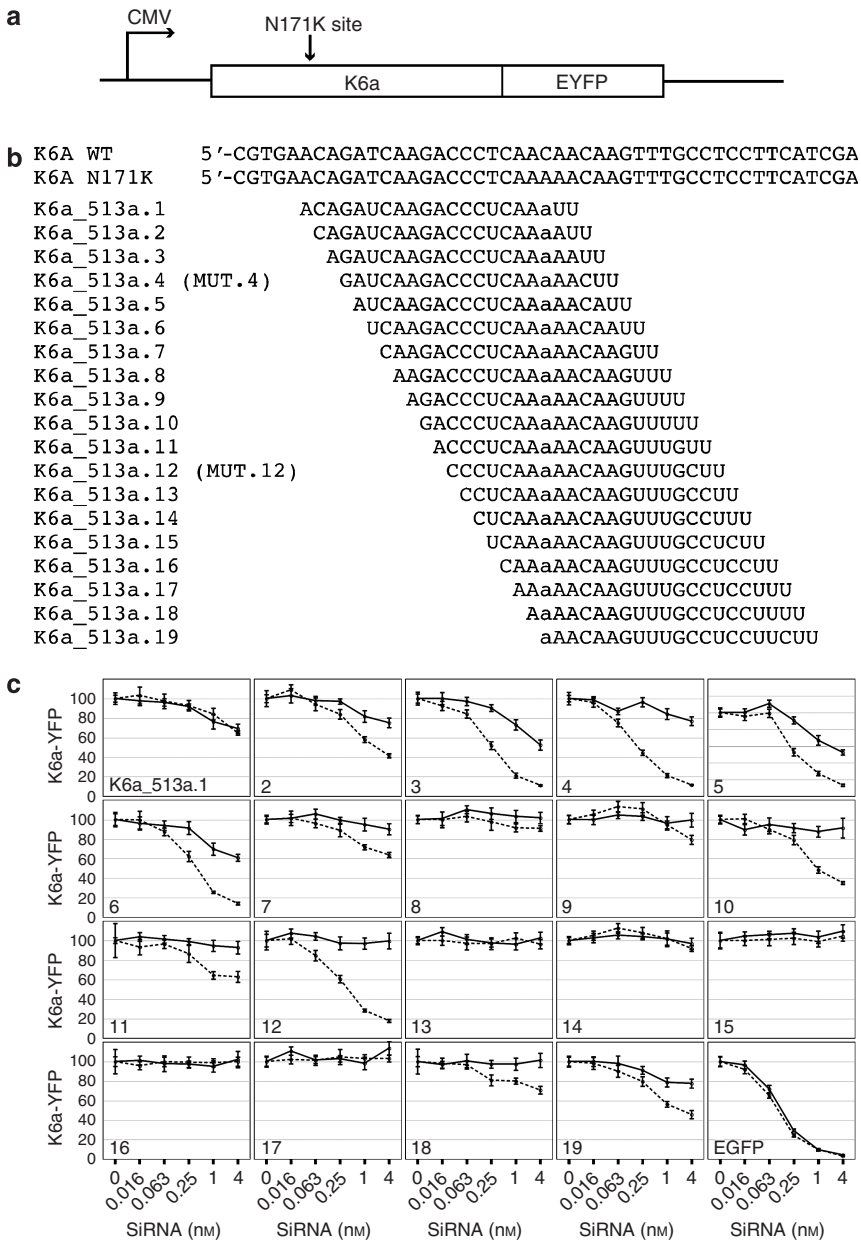

Figure 1. Complete siRNA sequence walk of the K6a-N171K single-nucleotide mutation site. (**a**) Schematic representation of the K6a/EYFP fusion expression constructs showing the N171K mutation. (**b**) SiRNAs (19 + 2 format) were designed and synthesized to screen all possible target sequences containing the single-nucleotide mutation (C513A) resulting in K6a-N171K. (**c**) Each K6a-N171K-specific siRNA was co-transfected in triplicate into 293FT tissue culture cells with 150 ng of either an expression vector containing K6a-N171K/EYFP fusion (dashed line) or a similar construct containing K6a-WT/EYFP (solid line). K6a/EYFP levels were determined by FACS analysis 48 hours following transfection. The data were normalized against data from cells transfected with NSC4 siRNA (nonspecific control).

expression plasmids without siRNAs (data not shown) or with irrelevant NSC4 siRNA were defective in keratin filament formation (only 16% of the cells contained predominantly keratin filaments). Co-transfection of cells with a mixture of wild-type and mutant expression plasmids and siRNAs that target mutant K6a (e.g. MUT.4 and MUT.12) rescued the ability to form keratin filaments (85 and 79% of the cells contained normal keratin filaments when co-transfected with MUT.4 and MUT.12, respectively).

As a control, cells were co-transfected with the wild-type/mutant expression plasmid mixture and the wild-type versions of the lead siRNAs (WT.4 and WT.12). Virtually, all of the cells contained keratin aggregates with few, if any, filaments when co-transfected with the wild-type inhibitors (92 and 97% of the cells contained predominantly aggregates when co-transfected with the wild-type/mutant expression plasmid mixture and WT.4 or WT.12 compared to 86% when co-transfected with mutant expression plasmid alone and

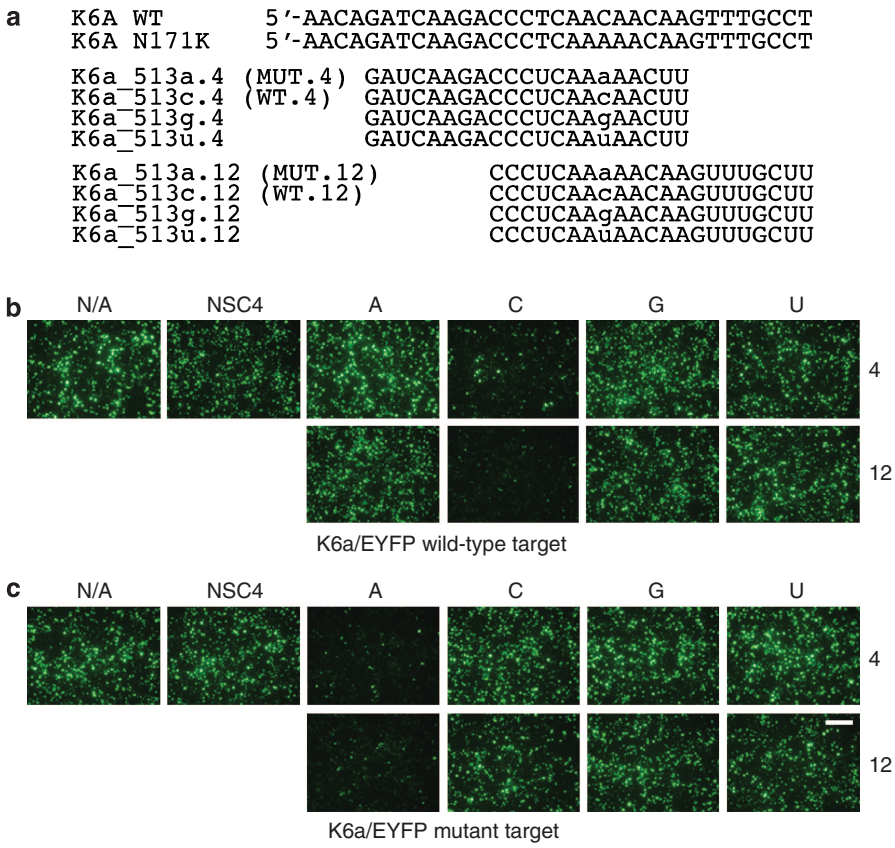

Figure 2. Exact sequence complementarity is necessary for inhibition of wild-type and mutant K6a expression by siRNAs at positions 4 and 12. (**a**) SiRNAs corresponding to positions 4 and 12 were designed and synthesized to target all possible nucleotides at mRNA position 513 (site of single-nucleotide mutation resulting in the N171K amino-acid change). Each siRNA (1 nM final concentration) was co-transfected in triplicate into 293FT tissue culture cells with 150 ng of either (**b**) pK6a-WT/EYFP (**c**) or pK6a-N171K/EYFP plasmid, and expression was visualized by fluorescence microscopy using a green fluorescent protein filter set. A representative image for each set of conditions is shown. Bar = 200 μm (bottom right panel).

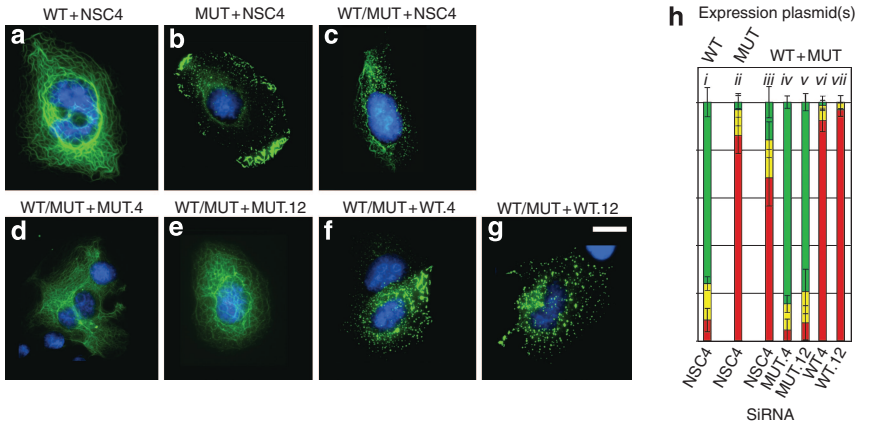

Figure 3. Treatment with K6a mutant-specific siRNA prevents keratin aggregates in a dominant-negative tissue culture model of PC. (**a–g**) PLC cells were co-transfected with pK6a-WT/EYFP, pK6a-N171K/EYFP, or a mixture of pK6a-WT/EYFP and pK6a-N171K/EYFP expression plasmids (designed to mimic the dominant-negative PC disease state) and 1 nM siRNA. (**a**) pK6a-WT/EYFP + NSC4; (**b**) pK6a-N171K/EYFP + NSC4; (**c**) pK6a-WT/EYFP + pK6a-N171K/EYFP + NSC4; (**d**) pK6a-WT/EYFP + pK6a-N171K/EYFP + MUT.4; (**e**) pK6a-WT/EYFP + pK6a-N171K/EYFP + MUT.12; (**f**) pK6a-WT/EYFP + pK6a-N171K/EYFP + WT.4; (**g**) pK6a-WT/EYFP + pK6a-N171K/EYFP + WT.12. Following a 48-hour incubation, the cells were fixed, stained with DAPI, and imaged by fluorescence microscopy using DAPI and green fluorescent protein filter sets (a representative image is shown; bar = 10 μm). (**h**) The slides were analyzed and a representative number of cells (see Materials and Methods) categorized as containing predominantly aggregates (red), predominantly filaments (green), or a mixture of aggregates and filaments (yellow). This experiment was repeated three times with similar results.

NSC4 siRNA). The increased keratin aggregation observed after treatment with siRNAs targeting wild-type K6a may be due to unintended silencing of endogenous K8 expressed in the PLC cells (see Discussion).

Differential labeling of wild-type and mutant K6a

Co-transfection of PLC cells with both wild-type and mutant K6a/EYFP expression constructs (both contain the same EYFP tag) results in bright yellow/green aggregates when visualized by fluorescence microscopy (Figure 3). To demonstrate further the single-nucleotide specificity of the MUT.4 and MUT.12 siRNAs, wild-type and mutant K6a were differentially labeled with tomato fluorescent protein (tdTFP) (Shaner *et al.*, 2004) and EYFP, respectively. Wild-type K6a tagged with tdTFP (pK6a-WT/tdTFP) was co-transfected with mutant K6a tagged with EYFP (pK6a-N171K/EYFP) into PLC cells. The ability to spectroscopically distinguish EYFP and tdTFP allows the visualization of faint red keratin filaments even in the presence of yellow/green keratin aggregates, which tend to be very bright. No cells that expressed only EYFP or tdTFP were found, suggesting that transient transfection of a given cell results in quantitative uptake and expression of both plasmids (data not shown). Similar results were observed with constructs containing plum fluorescent protein (Shaner *et al.*, 2005) substituted for tdTFP; however, the tdTFP label was brighter and therefore more easily visualized (data not shown). As seen in Figure 4, cells co-transfected with pK6a-WT/tdTFP and NSC4 siRNA were able to form keratin filaments (Figure 4a), whereas cells transfected with pK6a-N171K/EYFP resulted in aggregates (Figure 4b). In cells co-transfected with a mixture of pK6a-WT/tdTFP and pK6a-N171K/EYFP and NSC4 siRNA, red tdTFP-labeled filament structures and yellow/green EYFP-labeled aggregates were observed in some cells (Figure 4c), with the yellow/green aggregates often colocalizing along the red filaments (data not shown). Co-transfection of pK6a-WT/tdTFP and pK6a-N171K/EYFP with mutant-specific inhibitors (MUT.4 and MUT.12) resulted in robust knockdown of the K6a-N171K/EYFP protein without affecting K6a-WT/tdTFP expression; therefore, only red filaments were observed (Figure 4d and e). Co-transfection of pK6a-WT/tdTFP and pK6a-N171K/EYFP with wild-type-specific inhibitors (WT.4 and WT.12) resulted in specific knockdown of K6a-WT/tdTFP protein expression over K6a-N171K/EYFP, resulting in only yellow/green aggregates (Figure 4f and g). Reversal of the tags on the wild-type and mutant forms of K6a (i.e. pK6a-WT/EYFP and pK6a-N171K/tdTFP) resulted in the expected yellow/green filaments and red aggregates that were inhibited by their respective siRNAs (data not shown).

SiRNA-mediated downregulation of pre-existing K6a expression in human keratinocytes

Human HaCaT keratinocytes were transfected with K6a-specific siRNAs (WT.4 and WT.12) to test their ability to inhibit endogenous K6a (Figure 5). Ninety-six hours after transfection, cells were lysed and the protein extract was subjected to electrophoresis on a 4–12% bis-tris gel, transferred to nitrocellulose, and incubated with a K6a-specific antibody (Western blot analysis). It should be noted that HaCaT cells express K6a but not K6b, as determined by reverse transcriptase-PCR (F.J.D. Smith and W.H. Irwin McLean, unpublished data). A strong K6a band was seen in untreated HaCaT cells and those treated with the transfection reagent RNAiMAX, while a dramatic reduction in the amount of K6a protein was observed in cells treated with increasing concentrations of the K6a-specific siRNAs, WT.4 or WT.12

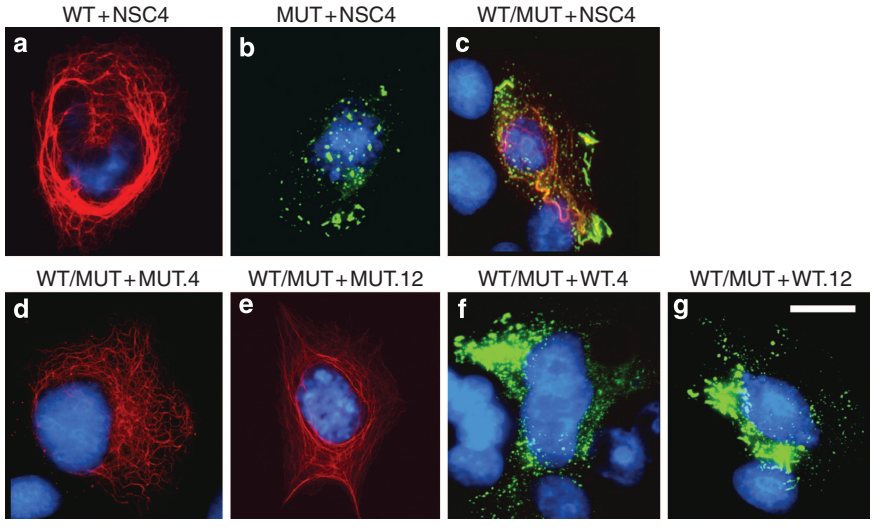

Figure 4. Differential labeling of wild-type and mutant K6a demonstrates single-nucleotide specificity in a PC disease model. PLC cells were co-transfected with pK6a-WT/tdTFP (fusion with tdTFP), pK6a-N171K/EYFP, or a mixture of pK6a-WT/tdTFP and pK6a-N171K/EYFP expression plasmids and 1 nM siRNA. (**a**) pK6a-WT/tdTFP + NSC4; (**b**) pK6a-N171K/EYFP + NSC4; (**c**) pK6a-WT/tdTFP + pK6a-N171K/EYFP + NSC4; (**d**) pK6a-WT/tdTFP + pK6a-N171K/EYFP + MUT.4; (**e**) pK6a-WT/tdTFP + pK6a-N171K/EYFP + MUT.12; (**f**) pK6a-WT/tdTFP + pK6a-N171K/EYFP + WT.4; (**g**) pK6a-WT/tdTFP + pK6a-N171K/EYFP + WT.12. After transfection (48 hours), the cells were fixed, stained with DAPI, and imaged by fluorescence microscopy using DAPI, green fluorescent protein, and rhodamine filter sets (a representative image is shown; bar = 10 μm). This experiment was repeated three times with similar results.

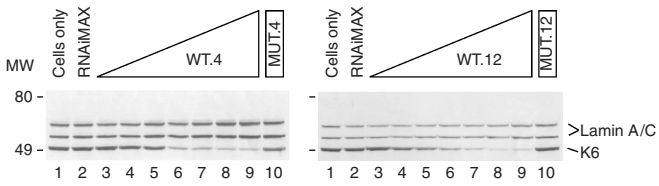

Figure 5. Inhibition of endogenous K6a expression in human keratinocytes. HaCaT cells were transfected with increasing concentrations of wild-type-specific siRNAs (lanes 3–9 containing 0, 1, 2, 5, 10, 15, and 20 nM WT.4 or WT.12) and 20 nM mutant-specific siRNAs (lane 10; MUT.4 or MUT.12). Lane 1 is a ''no treatment'' control. After 96 hours, cells were harvested and lysed in SDS-PAGE loading buffer, subjected to denaturing SDS-PAGE analysis, and electroblotted to nitrocellulose. K6a expression was detected by specific K6a antibody and visualized by the NBT/BCIP system. The blot was subsequently reacted with an antibody specific to lamin A/C to show equal lane loading and absence of generalized inhibition resulting from siRNA treatment.

(76 and 85% reduction, respectively). It should be noted that neither KA12 nor any other antibody currently available can distinguish K6a from K6b; however, since HaCaT cells only express K6a, the reduction in KA12 staining seen here is due to siRNA targeting that mRNA. A 35 and 10% reduction in K6a was observed upon treatment with mutant K6a-specific inhibitors MUT.4 and MUT.12, respectively. Lamin A/C expression is not inhibited by K6a-specific siRNA treatment and was therefore used as a control to correct for differences in sample loading. The wild-type K6a-specific knockdown was confirmed at the mRNA level by Northern blot analysis (data not shown). These results indicate that the wild-type K6a siRNAs can inhibit endogenous K6a under conditions where mutant K6a siRNAs have little effect, further demonstrating single-nucleotide specificity.

Delivery and effectiveness of siRNAs in mouse footpad skin

To perform translational research with the K6a inhibitors in an *in vivo* bioluminescence mouse model, a bicistronic reporter gene/K6a (wild type or mutant) plasmid (Figure 6a) was prepared that contains the firefly luciferase and K6a open reading frames separated by the foot and mouth disease virus 2A element (Cao *et al.*, 2005b; Wang *et al.*, 2007). As expected from the results using the EYFP reporter constructs (Figures 1–4), both MUT.4 and MUT.12 siRNAs potently and selectively inhibited mutant K6a expression as measured by luciferase activity (Figure 6b). The IC_{50} values for MUT.4 and MUT.12 against the fluc/K6a constructs were identical to those against the K6a/EYFP constructs determined by FACS (Figure 1). These siRNAs were next intradermally injected into female FVB mouse footpads. Mouse footpad skin was chosen over other mouse skin in part due to its greater thickness, the absence of hair follicles, ease of access, and relevance to PC (Wang *et al.*, 2007). At the indicated time points after gene transfer, luciferin was injected intraperitoneally and the amount of light emitted as a result of fLuc expression was determined using the IVIS *in vivo* imaging system (Figure 6c shows the image at the 24-hour time point). The non-invasive nature of this approach allows real-time monitoring of reporter gene expression over multiple time points in the same animals, thereby minimizing the number of mice required and maximizing the amount and quality of data obtained. Paws co-injected with the bicistronic target containing mutant K6a along with mutant-specific siRNAs (MUT.4 and MUT.12) show weak luciferase activity, compared with control paws co-injected with pUC19 plasmid or NSC4. Figure 6d shows the quantification over 3 days, the bolded line representing the average of five mice per treatment group. Although there is variability in the data, there is a clear decrease in luciferase activity in the paws co-injected with specific inhibitor compared with control paws, indicating that these inhibitors are effective in intact skin.

DISCUSSION

Dominant-negative mutations result in a variety of diseases because of gain of toxic function by the defective protein. Many of these genes encode essential proteins; therefore, treatment would necessitate selective inhibition of mutant gene expression without affecting wild-type expression. The ability of siRNAs to discriminate between highly homologous sequences, even single-nucleotide changes, theoretically allows for the treatment of any disease caused by a dominant mutation, assuming delivery challenges can be overcome and that sufficient wild-type protein is produced from the unaffected gene.

Successful allele-specific silencing methods utilizing RNAi technology to discriminate single-nucleotide mutations have been reported recently, targeting either the mutation itself (Brummelkamp *et al.*, 2002; Ding *et al.*, 2003; Schwarz *et al.*, 2006; Dykxhoorn *et al.*, 2006b) or a single-nucleotide polymorphism site associated with only the mutant mRNA allele (Miller *et al.*, 2003). In most of these studies, siRNAs were designed such that the mutation was aligned with the center (positions 9–11 from the 5′ end) of the guide strand based on the observation that this region directs mRNA cleavage (Elbashir *et al.*, 2001). As in the study reported by Schwarz *et al.* (2006), we identified effective inhibitors by testing all possible siRNAs (19 + 2 format) against a specific single-nucleotide mutation site. The selectivity conferred by the mismatch between wild-type mRNA and MUT.10 siRNA (located at position 10 from the 5′ end of the guide strand; Figure 1) is consistent with the position-dependent single-nucleotide selectivity observed in previous studies (Brummelkamp *et al.*, 2002; Ding *et al.*, 2003; Miller *et al.*, 2003; Schwarz *et al.*, 2006; Dykxhoorn *et al.*, 2006b). However, placement of the mismatch at positions 9 and 11 of the guide strand showed moderate activity against the mutant mRNA (21 and 37% reduction, respectively), with no effect on wild-type expression.

In addition to MUT.10, our screen identified two other highly selective and potent inhibitors, MUT.4 and MUT.12. Each of these demonstrated higher potency than MUT.10, while retaining selectivity, reducing mutant gene expression by 88 and 82%, respectively. MUT.4 reduced wild-type expression by 23%, whereas MUT.12 had no effect (Figure 1). These inhibitors contain the single-nucleotide mutation located at positions 4 and 12 from the 5′ end of the guide strand, respectively. Schwarz *et al.* (2006) reported that siRNAs with the single-nucleotide mismatch at positions 9,

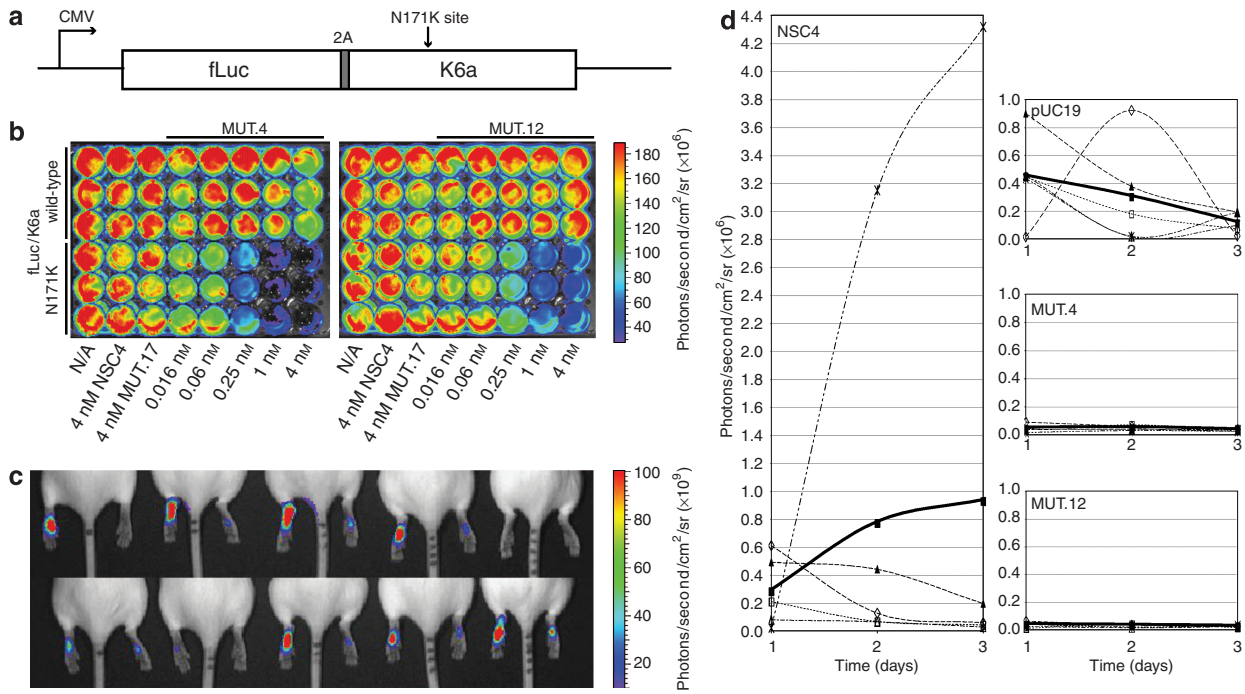

Figure 6. Inhibition of K6a (N171K)/fLuc reporter gene expression by specific siRNAs in a mouse footpad skin model. (**a**) Schematic representation of the fLuc/K6a bicistronic expression constructs showing the N171K site and the foot and mouth disease virus 2A element (shaded). (**b**) 293FT cells were co-transfected in triplicate with fLuc/K6a expression constructs in a 48-well plate format. After transfection (48 hours), luciferin was added and light emitted was visualized using the Xenogen IVIS100 *in vivo* imaging system. Red color represents highest luciferase expression and purple lowest. (**c**) Mice (five per group) were co-injected intradermally with 10 μg pK6a-N171K/fLuc expression plasmid and 10 μg of pUC19 plasmid (top panel, left paw), NSC4 siRNA (bottom panel, left paw), MUT.4 siRNA (top panel, right paw), or MUT.12 siRNA (bottom panel, right paw). After 24 hours, luciferase expression in the footpads was determined following intraperitoneal luciferin injection by whole-animal imaging using the Xenogen IVIS200 *in vivo* system. (**d**) Quantification of luciferase activity in treated mice (24, 48, and 72 hours) was performed using LivingImage software and demonstrates reduction in fLuc signals in paws treated with mutant-specific K6a siRNA compared with controls (pUC19 plasmid and NSC4 siRNA). Bolded line shows averaged results for each treatment.

10, 12, 13, 14, and 16 from the 5′ end of the guide strand were able to discriminate between the mutant and wild-type SOD1 alleles. Although our results demonstrating that mismatches at positions 10 and 12 also show allele-specific discrimination, our data indicate that a mismatch at position 4 can discriminate as well. The siRNAs designed to target the K6a gene with mismatches at positions 9, 13, 14, and 16 were inactive against both the mutant and wild-type alleles. The reasons for these discrepancies are not known, and further experiments are needed to elucidate the mechanisms involved.

It has been suggested that to gain single-nucleotide selectivity, a purine–purine mismatch is required between the siRNA and the wild-type sequence (Dykxhoorn *et al.*, 2006b). A systematic study, in which all possible single-nucleotide mismatches relative to a single potent siRNA were monitored, demonstrated that any mismatch at position 10 (more so than at any other position) significantly reduced silencing, regardless of the mismatch composition (Du *et al.*, 2005). In this study, all possible mismatches between siRNAs (at positions 4 and 12) and K6a wild-type and mutant targets were analyzed. Only siRNAs with exact complementarity blocked gene expression, whereas all single-nucleotide mismatches abrogated silencing, regardless of composition (Figure 2b and see Figure S2 for quantitative data).

The levels of mutant keratin may not need to be completely blocked and indeed may only need to be reduced by 50% to show a phenotype reversal in PC (Cao *et al.*, 2001; Wong *et al.*, 2005) or EBS, a skin disorder closely related to PC (Cao *et al.*, 2001). Like PC, EBS is a dominant-negative keratin disorder, in which K5 (similar to K6) or K14 (similar to K16 and K17) is mutated and is characterized by skin fragility resulting in blisters caused by little or no trauma (Irvine and McLean, 1999). In an attempt to generate an EBS mouse model that mimics the dominant-negative disease at the genetic level and also exhibits the EBS phenotype, Roop and co-workers introduced a mutant K14 gene along with a neo cassette in intron I (Cao *et al.*, 2001). These heterozygous mice appeared normal, showing no signs of blistering. Semiquantitative reverse transcriptase-PCR analysis showed mutant K14 levels at 50% of wild-type K14. Removal of the neo cassette resulted in equivalent levels of mutant and wild-type K14 expression as well as a disease phenotype, suggesting that as little as 50% knockdown of the mutated keratin may be sufficient to allow a normal phenotype.

Consistent with the EBS mouse model, in which complete removal of mutant protein may not be necessary for a therapeutic effect, our tissue culture model (developed to mimic PC) demonstrated that treatment with K6a mutant-selective siRNA results in a normal phenotype. Co-transfec-

tion of MUT.10 (data not shown), which was less efficient than MUT.4 and MUT.12, demonstrated similar results, further suggesting that incomplete inhibition may be sufficient to essentially ''heal'' the cell by allowing efficient formation of filaments.

Skin represents an attractive target for nucleic acid-based therapies owing to its ease of accessibility and the ability to locally deliver therapeutic agents (Pines *et al.*, 2001; Khavari *et al.*, 2002). Although the stratum corneum (the dead cornified, outermost barrier layer of the epidermis) may be difficult to penetrate, once nucleic acid is intradermally delivered, keratinocytes are capable of taking up and expressing naked DNA within hours as demonstrated in mouse, pig, and human skin (Hengge *et al.*, 1995; Hengge *et al.*, 1996; Sawamura *et al.*, 2002). We have recently shown that intradermal injection of a bicistronic luciferase-EGFP expression plasmid into mouse footpads results in luciferase expression, which is robustly silenced upon co-injection with reporter-specific chemically stabilized or unmodified siRNA (Wang *et al.*, 2007). These data are consistent with previous reports demonstrating expression of naked plasmid DNA *in vivo*, and further suggest that naked, unmodified siRNAs can be taken up by and function efficiently in skin.

Despite the rapid growth of RNAi technology, off-target effects are not well understood and remain a concern (Dykxhoorn and Lieberman, 2006). The K6a N171 region is conserved among many type II keratins; however, the single-nucleotide selectivity observed between wild-type and mutant K6a suggests that our lead inhibitors will have little or no effect on wild-type keratin expression. Owing to the high-sequence conservation surrounding the K6a N171 site with other keratins, if single nucleotide changes are tolerated by the RISC complex, there may be downregulation of other members of the keratin gene/protein family. Indeed, transfection of the wild-type versions of the lead inhibitors (WT.4 and WT.12) into HaCaT and PLC cells showed inhibition of a number of endogenous proteins in addition to K6a, including K8. K5 was partially inhibited by MUT.4, but was not affected by WT.12 (data not shown). As noted previously, K6b is not expressed in HaCaT cells; however, owing to the exact sequence identity with K6a at the target site, K6b is expected to be inhibited upon treatment with wild-type K6a inhibitors. Of particular importance to developing these inhibitors as potential therapeutics, the lead *mutant-specific* K6a siRNAs showed no off-target effects on wild-type keratin expression nor on any other proteins on silver-stained two-dimensional gels (data not shown), under conditions in which WT.4 and WT.12 siRNAs potently downregulated endogenous K6a expression. These data are consistent with the single-nucleotide specificity observed in other experiments (Figures 1–5 and data not shown).

K8 and K18 are not expressed in HaCaT cells, but together form the major intermediate filament network in simple epithelial cells (Lane, 1993), including the PLC cells used in this report (Woll *et al.*, 2005). Sequence alignment (see Figure S3) shows exact identity between K8 and K6a in the region surrounding N171. Inhibition of K8 by WT.4 and WT.12 siRNAs may account for the decrease in the number of cells with keratin filaments when PLC cells are treated with these inhibitors (Figure 3b, bars *vi* and *vii*). One possible explanation for the filaments observed in cells transfected with the wild-type and mutant K6a expression plasmids is that the K8/K18 network incorporates the wild-type K6a-EYFP fusion protein. Therefore, the decrease observed in intermediate filaments upon co-transfection with the wild-type inhibitors may be due to knockdown of both wild-type K6a and K8, thereby allowing mutant K6a to more efficiently pair with K18 and disrupt filament formation. Although the wild-type inhibitors decrease expression of multiple keratins, it is important to note that the lead mutant-specific inhibitors only target the N171K form of K6a and have little or no effect on wild-type keratin expression.

The siRNAs reported in this study did not contain modifications, which can increase stability (resistance to nucleases) or enhance delivery. Unmodified siRNAs typically have half-lives of less than 20 minutes in serum, as analyzed by PAGE (Chiu and Rana, 2003; Czauderna *et al.*, 2003; Layzer *et al.*, 2004; Morrissey *et al.*, 2005), although longer-lived RNA duplexes have been reported (Braasch *et al.*, 2003). Although chemical modifications can greatly enhance stability in serum, the increase in half-life does not always result in a corresponding increase in functional activity (Layzer *et al.*, 2004). In addition, it should be noted that many of the *in vivo* studies demonstrating disease protection were performed using unmodified inhibitors (Giladi *et al.*, 2003; McCaffrey *et al.*, 2003; Song *et al.*, 2003; Wang *et al.*, 2005; Wesche-Soldato *et al.*, 2005; Dykxhoorn *et al.*, 2006a), suggesting that serum stability is only one consideration in developing an effective therapeutic. Indeed, owing to the rapid clearance of siRNAs by the renal system (elimination half-life of 6 minutes; Soutschek *et al.*, 2004), the identification of modifications that allow directed delivery may be of greater importance than enhanced stability for development of siRNA-based therapeutics.

A number of chemically modified mutant and wild-type K6a siRNAs were tested in tissue culture and mouse models and were found to have potencies similar to those of unmodified inhibitors (data not shown). Chemical modifications on the guide strand of the duplex that improve nuclease resistance often enhance thermodynamic stability of target hybridization, which in some instances resulted in loss of single-nucleotide specificity. In this application, chemical modifications for nuclease resistance are not expected to be advantageous, as inhibitors are locally delivered via intradermal injection to the affected skin, and unmodified siRNAs may achieve better selectivity between wild-type and mutant transcripts.

The potency and selectivity of the lead K6a siRNAs developed against the N171K mutation site in K6a (MUT.4 and MUT.12) indicate that these may be ideal candidates for clinical trials if efficient delivery can be achieved. We have shown that the wild-type siRNA counterparts can efficiently inhibit endogenous wild-type K6a expression in human keratinocytes, whereas mutant-specific siRNAs show little or no effect (Figure 5). We have also demonstrated the ability to knock down EGFP expression in a transgenic EGFP mouse

model by intradermal injection of unmodified EGFP-specific siRNAs into mouse footpads (unpublished data). Taken together, these data suggest that siRNA injection is a potentially viable approach for patients suffering from dominant-negative skin disorders, including PC. Further investigation is needed to determine the extent of siRNA distribution and the ability to inhibit endogenous gene expression in intact skin.

MATERIALS AND METHODS

Design of siRNA

siRNAs (19 + 2 format; 19-nucleotide duplex with two 3′ uracyl nucleotide overhangs) were synthesized by Thermo Fisher Scientific, Dharmacon Products (Lafayette, CO) to screen all possible target sequences containing the N171K mutation previously described in two multigeneration families and one sporadic case of PC (Lin *et al.*, 1999; Smith *et al.*, 1999). This C > A point mutation occurs at position 513 in the K6a coding sequence, numbering from the A in the initiating ATG codon (gene name *KRT6A*, GenBank accession no. NM 005554). The sense and antisense strands for K6a_513a.1 are 5′-ACAGAUCAAGACCCUCAAAUU-3′ and 5′-P-UUUGAGG GUCUUGAUCUGUUU-3′, respectively. Sense and antisense strands for siRNAs K6a_513a.2 through K6a_513a.19 were designed similarly, and the sense strands are listed in Figure 1. The sense strands for the wild-type counterparts are listed in Supplementary material (see Figure S1). The SMARTselected™ EGFP sequences for the sense and antisense strands are 5′-GCACCAUCUUCUUCAAG GAUU and 5′-P-UCCUUGAAGAAGAUGGUGCUU, respectively. The NSC4 siRNA (inverted *β*-galactosidase sequence) sense and antisense sequences are 5′-UAGCGACUAAACACAUCAAUU and 5′-P-UUGAUGUGUUUAGUCGCUAUU, respectively (Thermo Fisher Scientific, Dharmacon Products, catalog no. D-001210).

Design of expression plasmids

K6a-EYFP fusion constructs. To generate expression constructs for mutant (N171K) and wild-type K6a fusion proteins tagged with EYFP, an *Eco*RI–*Xho*I fragment consisting of full-length human K6a insert (contains 5′ and 3′ untranslated regions (UTR)) from IMAGE clone 3639270 (MRC Geneservice, Cambridge, UK) was subcloned into pcDNA3 (Invitrogen, Carlsbad, CA) generating clone 128. The stop codon was replaced by a *Bam*HI site (underlined) for in-frame cloning into pEYFP-N1 (Clontech, Mountain View, CA) using the QuickChange site-directed mutagenesis system (Stratagene, La Jolla, CA) with the following primers: K6a.XBAM.F (5′-AGCTATAAG CACTCGGATCCGTCTGCTAGCTC-3′) and K6a.XBAM.R (5′-GAGC TAGCAGACGGATCCGAGTGCTTATAGCT-3′). Similarly, the N171K mutation was introduced using the following primers: N171K.L (TC AAGACCCTCAAAAACAAGTTTGC-3′) and N171K.R (5′GCAAACTT GTTTTTGAGGGTCTTGA-3′. DNA oligonucleotides were obtained from Integrated DNA Technologies (Coralville, IA) and from MWG Biotech (Ebersberg, Germany). The 2.5 kb *Hin*dIII/*Not*I-digested PCR DNA fragments were further subcloned into pcDNA5/FRT (Invitrogen) generating pTD100 and pTD101. The K6a 3′UTR was cloned downstream of EYFP into pTD100 and pTD101 by PCR amplification using the following primers: K6a.3′UTR.NOT.U (5′-AAGGAAAAAAGCGGCCGCAGGAAGAGCTATAAGCACT-3′) and K6a.3′UTR.D (5′-AAAGAAGGGCCCTCGAGGCAAAGAGCGAAGA GCACAG-3′), adding an upstream *Not*I site (underlined). The PCR product was inserted into the pCRII-TOPO vector for amplification using the TOPO TA cloning system (Invitrogen). The insert was removed by *Not*I digestion (downstream *Not*1 site was located in the pCRII-TOPO vector) and cloned into *Not*I-linearized pTD100 and pTD101, resulting in the expression plasmids pTD103 (K6a-WT/ EFYP) and pTD104 (K6a-N171K/EYFP), respectively. Clones were verified by sequence analysis.

K6a-fLuc fusion constructs. To generate bicistronic constructs expressing both firefly luciferase and mutant (or wild type) K6a, the foot and mouth disease virus 2A element was used. The foot and mouth disease virus 2A sequence results in pseudotermination of the polypeptide encoded in the first open reading frame (fLuc in this case), and then without disengaging from the mRNA, the second open reading frame (K6a) is translated (Donnelly *et al.*, 2001; de Felipe *et al.*, 2006). The K6a-EYFP-3′UTRs of pTD103 and pTD104 (*Hin*dIII/*Pme*I digested followed by Klenow polymerase ''fill-in'' to create ''blunt ends'') were cloned into the *Bam*HI/*Hin*dIII sites of pL2G (Cao *et al.*, 2005a) (calf intestinal alkaline phosphatase-treated and ''blunt-ended'' by Klenow polymerase), resulting in plasmids pTD106 and pTD107. The 2A expression element, between the fLuc and K6a coding regions in pTD106, was corrected by quick-change mutagenesis using the following forward and reverse primers: L2K.2a.F (5′-CCAACCCTGGGCCCGGGATCCACCGGCCGGTCG CCACCATGGCCAGCACATCCACCAC-3′) and L2K.2a.R (5′-GTGGT GGATGTGCTGGCCATGGTGGCGACCGGCCGGTGGATCCCGG GCCCAGGGTTGG-3′), respectively. The resulting *Sgr*AI/*Bst*EII PCR DNA fragment (700 bp) containing the corrected 2A region was inserted into pTD106 and pTD107, resulting in pTD110 and pTD111. The region coding for EYFP in pTD110 was deleted by quick-change mutagenesis using the forward and reverse primers: L2K.EYFP.F (5′-CAGCAGGAAGAGCTATAAGCACTAAAGTGCGTC TGCTAGCTCTCG-3′) and L2K.EYFP.R (5′CGAGAGCTAGCAGA CGCACTTTAGTGCTTATAGCTCTTCCTGCTG-3′), respectively. The *Kpn*I/*Eco*RI fragment (1,200 bp) without EYFP was cloned into pTD110 and pTD111, resulting in pTD114 and pTD115. Clones were verified by sequence analysis.

K6a/tdTFP fluorescent protein constructs. The gene encoding tdTFP was PCR-amplified from pRSET (td-tomato, generously provided by Roger Tsien, UCSD) using the primers YFP.BAMHI.U (5′-TCGGATCCACCGGTCGCCACCATGGTGAGCAAGGGCGAGG-3′) and YFP.ECORV.D (5′-TGGATATCGCTTTACTTGTACAGCTCGT CCATGCC-3′), adding an upstream *Bam*HI site and a downstream *Eco*RV site (sites underlined). The PCR product was inserted into the pCRII-TOPO vector for amplification using the TOPO TA cloning system (Invitrogen). The insert was removed and cloned into *Bam*HI/ *Eco*RV-digested pK6a-WT/EYFP and pK6a-N171K/EYFP, resulting in the expression plasmids pTD128 (K6a-WT/tdTFP) and pTD129 (K6a-N171K/tdTFP), respectively. Clones were verified by sequence analysis.

Cell culture

Human 293FT embryonic kidney cells (Invitrogen), human HaCaT keratinocytes (Boukamp *et al.*, 1988), and human PLC hepatoma cells (ATCC CRL8024) were maintained in DMEM (CAMBREX/ BioWhittaker, Walkersville, MD) with 10% fetal bovine serum

(HyClone, Logan, UT), supplemented with 2 mM L-glutamine and 1 mM sodium pyruvate (growth media).

Transient transfections of expression plasmids and siRNA

293FT transfections. The day before transfection, 293FT cells were seeded at 8×10^4 cells/well in a 48-well plate resulting in 80% cell confluency at the time of transfection. Cells were transfected with Lipofectamine 2000 (Invitrogen) following the manufacturer's instructions. Cells were co-transfected (in triplicate) with a mixture of 150 ng expression plasmid, siRNA (final concentration 0.016–4 nM per transfection), and pUC19 (to give a final nucleic acid concentration of 400 ng per transfection), diluted to 25 μl in optiMEM medium (Invitrogen). One microliter of Lipofectamine 2000 was diluted in 25 μl of optiMEM medium and incubated at room temperature for 5 minutes. This mixture was added to the nucleic acid and incubated for 20 minutes at room temperature, before addition to the plated cells.

Forty-eight hours following transfection, the cells were treated with 120 μl trypsin (CAMBREX/BioWhittaker) for 15 minutes at 37°C. Growth medium (120 μl) was added and the sample was vigorously mixed by pipetting. Each sample was diluted four-fold with PBS and analyzed for EYFP expression by FACS (BD FACScan, BD Biosciences, San Jose, CA) using the instrument's channel FL1 (530 nm emission filter). A total of 5,000 cells per transfection were analyzed. The data were generated by gating the cells and determining the percentage of cells that dropped below the gate with and without siRNA treatment. All data collected from cells treated with specific and nonspecific siRNA were normalized to the value obtained from cells transfected with expression plasmid, but no siRNA. Data obtained from cells treated with the NSC4 siRNA were used to correct data obtained from cells treated with specific siRNAs. Error bars reported for this and all other experiments represent standard deviations.

Alternatively, to measure firefly luciferase expression, 48 hours after transfection, 50 μl of 3 mg/ml luciferin (in PBS) was added to each well and incubated at room temperature for 3–5 minutes. The entire plate was imaged for 20 seconds using the IVIS *in vivo* imaging system (Xenogen Corp., Alameda, CA).

PLC transfections. PLC hepatocytes were seeded at 4×10^4 cells/well as described above for 293FT cells and co-transfected with wild type, mutant, or a 3:7 mixture of wild-type and mutant K6a expression plasmids tagged with either EYFP or tdTFP (200 ng total) and 1 nM siRNA (final concentration), supplemented with pUC19 to give a final nucleic acid concentration of 400 ng per transfection. Twenty-four hours after transfection, the cells were treated with 120 μl trypsin at 37°C for 15 minutes. Growth medium (880 μl) was added and the cells were vigorously mixed by pipetting and 500 μl was transferred to four-well chamber slides (Labtek II, Nunc, Rochester, NY). Forty-eight hours after transfection, the growth medium was removed and the cells were washed twice with PBS and fixed with 500 μl ice-cold methanol/acetone (1:1) at room temperature for 5 minutes. The methanol/acetone was removed and the slides were allowed to dry. The cells were stained with 500 μl of 0.4 μg/ml DAPI (Sigma, St Louis, MO) in PBS, mounted with Histomount (National Diagnostics, Atlanta, GA), and imaged by fluorescence microscopy (Zeiss Axioplan 2, ID 203090, with FluoArc equipped with filter sets for DAPI, green fluorescent protein, and rhodamine). The slides were analyzed and at least 20 cells per transfection were categorized as containing predominantly aggregates, predominantly filaments, or a mixture.

Human keratinocyte transfections. HaCaT keratinocytes were transfected with RNAiMAX (Invitrogen) according to the manufacturer's instructions for ''reverse transfection.'' Mutant- or wild-type-specific siRNA (final concentration 0–20 nM), supplemented with EGFP siRNA to give a final total siRNA concentration of 20 nM, was diluted in 50 μl optiMEM medium in a well of a 48-well plate. One microliter of RNAiMAX lipofectamine (Invitrogen) was diluted in 50 μl of optiMEM medium and immediately added to the nucleic acid solution and left for 20 minutes at room temperature. Trypsinized HaCaT cells (2×10^4 cells in 500 μl) were then added to the well and gently mixed before incubation.

Western blot analysis

HaCaT keratinocytes (96 hours post-transfection) were washed twice with PBS, lysed with NuPAGE 1 × loading dye/solubilization buffer (lithium dodecyl sulfate buffer; Invitrogen), supplemented with 100 mM dithiothreitol, subjected to electrophoresis in NuPAGE Novex 4–12% bis-tris gels (Invitrogen), and electroblotted to nitrocellulose (Invitrogen). K6a expression was detected by KA12 primary antibody (Progen Biotechnik GmbH, Heidelberg, Germany) and goat anti-mouse IgG-alkaline phosphatase secondary antibody (Santa Cruz Biotechnology, Santa Cruz, CA) and visualized by the NBT/BCIP system (Promega, Madison, WI). The blot was subsequently reacted with a primary antibody specific to lamin A/C (Upstate USA Inc., Charlottesville, VA) to show equal lane loading and absence of generalized inhibition resulting from siRNA treatment. Band intensities were quantified using ImageJ software (http://www.rsb.info.nih.gov/ij/). The reported K6a values were generated by dividing normalized K6a band intensites by the average of the normalized lamin A and lamin C band intensities.

Mice

Six-week-old female FVB mice were obtained from the animal facility of Stanford University. Animals were treated according to the Guidelines for Animal Care of both NIH and Stanford University.

Mouse footpad injections and *in vivo* imaging

Mouse footpad injections were performed as described previously (Wang *et al.*, in press). In a typical experiment, a total volume of 50 μl PBS containing 10 μg siRNA and 10 μg of expression plasmid was intradermally injected (28-gauge needle; Bectin Dickson and Company, Franklin Lakes, NJ) into a mouse footpad. At the indicated time points, the mice were imaged 10 minutes after intraperitoneal injection of luciferin (100 μl of 30 mg/ml luciferin; 150 mg/kg body weight). Mice were sedated using isoflurane and live anesthetized mice were imaged using the IVIS100 *in vivo* imaging system (Xenogen Corp.). The resulting light emission was quantified using LivingImage software (Xenogen Corp.), written as an overlay on Igor image analysis software (WaveMetrics Inc., Lake Oswego, OR). Raw values are reported as photons/second/cm^2/sr.

CONFLICT OF INTEREST

Dr Contag is the founder of Xenogen Corp. Drs Kaspar, Hickerson, Smith, and McLean have filed patents relating to siRNA therapy for PC.

ACKNOWLEDGMENTS

We thank Roger Tsien (UCSD) for generously providing the tomato and plum fluorescent protein constructs, Helen Blau (Stanford University) and members of her lab for instruction and use of her fluorescence microscope, and Qian Wang and Tim Doyle of the Contag laboratory for excellent help with the animal imaging. We thank Heini Ilves, Rebecca Kaspar, and Robert Kaspar for technical assistance. We thank Brian Johnston and other members of Somagenics for use of their FACScan and other equipment. We thank Alexander Vlassov and Emilio Gonzalez-Gonzalez for critical reading of the manuscript. This project is supported by NIH Grant no. R24CA92862 (C.H.C.) and a Career Development Fellowship from PC-Project (F.J.D.S.). Finally, we are grateful for the generous support, collegiality, and useful suggestions from members of PC-Project and The International Pachyonychia Congenita Consortium (IPCC) and in particular, Rudolf Leube, for providing K6a expression plasmids.

SUPPLEMENTARY MATERIAL

Figure S1. Complete siRNA sequence walk of K6a-N171K single-nucleotide mutation.

Figure S2. Exact sequence complementarity is necessary for inhibition of wild-type and mutant K6a expression by siRNAs at positions 4 and 12.

Figure S3. Sequence alignment of keratins in the N171 region.

REFERENCES

Bonifas JM, Rothman AL, Epstein EH Jr (1991) Epidermolysis bullosa simplex: evidence in two families for keratin gene abnormalities. *Science* 254:1202–5

Boukamp P, Petrussevska RT, Breitkreutz D, Hornung J, Markham A, Fusenig NE (1988) Normal keratinization in a spontaneously immortalized aneuploid human keratinocyte cell line. *J Cell Biol* 106:761–71

Braasch DA, Jensen S, Liu Y, Kaur K, Arar K, White MA *et al.* (2003) RNA interference in mammalian cells by chemically-modified RNA. *Biochemistry* 42:7967–75

Brummelkamp TR, Bernards R, Agami R (2002) Stable suppression of tumorigenicity by virus-mediated RNA interference. *Cancer Cell* 2: 243–7

Cao T, Longley MA, Wang XJ, Roop DR (2001) An inducible mouse model for epidermolysis bullosa simplex: implications for gene therapy. *J Cell Biol* 152:651–6

Cao YA, Bachmann MH, Beilhack A, Yang Y, Tanaka M, Swijnenburg RJ *et al.* (2005a) Molecular imaging using labeled donor tissues reveals patterns of engraftment, rejection, and survival in transplantation. *Transplantation* 80:134–9

Cao YA, Bachmann MH, Beilhack A, Yang Y, Tanaka M, Swijnenburg RJ *et al.* (2005b) Molecular imaging using labeled donor tissues reveals patterns of engraftment, rejection, and survival in transplantation. *Transplantation* 80:134–9

Chiu YL, Rana TM (2003) siRNA function in RNAi: a chemical modification analysis. *RNA* 9:1034–48

Coulombe PA, Hutton ME, Letai A, Hebert A, Paller AS, Fuchs E (1991) Point mutations in human keratin 14 genes of epidermolysis bullosa simplex patients: genetic and functional analyses. *Cell* 66: 1301–11

Czauderna F, Fechtner M, Dames S, Aygun H, Klippel A, Pronk GJ *et al.* (2003) Structural variations and stabilising modifications of synthetic siRNAs in mammalian cells. *Nucleic Acids Res* 31:2705–16

de Felipe P, Luke GA, Hughes LE, Gani D, Halpin C, Ryan MD (2006) *E unum pluribus*: multiple proteins from a self-processing polyprotein. *Trends Biotechnol* 24:68–75

Ding H, Schwarz DS, Keene A, Affar el B, Fenton L, Xia X *et al.* (2003) Selective silencing by RNAi of a dominant allele that causes amyotrophic lateral sclerosis. *Aging Cell* 2:209–17

Donnelly ML, Luke G, Mehrotra A, Li X, Hughes LE, Gani D *et al.* (2001) Analysis of the aphthovirus 2A/2B polyprotein 'cleavage' mechanism indicates not a proteolytic reaction, but a novel translational effect: a putative ribosomal 'skip'. *J Gen Virol* 82:1013–25

Du Q, Thonberg H, Wang J, Wahlestedt C, Liang Z (2005) A systematic analysis of the silencing effects of an active siRNA at all single-nucleotide mismatched target sites. *Nucleic Acids Res* 33:1671–7

Dykxhoorn DM, Lieberman J (2006) Knocking down disease with siRNAs. *Cell* 126:231–5

Dykxhoorn DM, Palliser D, Lieberman J (2006a) The silent treatment: siRNAs as small molecule drugs. *Gene Therapy* 13:541–52

Dykxhoorn DM, Schlehuber LD, London IM, Lieberman J (2006b) Determinants of specific RNA interference-mediated silencing of human beta-globin alleles differing by a single nucleotide polymorphism. *Proc Natl Acad Sci USA* 103:5953–8

Elbashir SM, Martinez J, Patkaniowska A, Lendeckel W, Tuschl T (2001) Functional anatomy of siRNAs for mediating efficient RNAi in *Drosophila melanogaster* embryo lysate. *EMBO J* 20:6877–88

Giladi H, Ketzinel-Gilad M, Rivkin L, Felig Y, Nussbaum O, Galun E (2003) Small interfering RNA inhibits hepatitis B virus replication in mice. *Mol Ther* 8:769–76

Hengge UR (2006) Gene therapy progress and prospects: the skin—easily accessible, but still far away. *Gene Therapy* 13:1555–63

Hengge UR, Chan EF, Foster RA, Walker PS, Vogel JC (1995) Cytokine gene expression in epidermis with biological effects following injection of naked DNA. *Nat Genet* 10:161–6

Hengge UR, Walker PS, Vogel JC (1996) Expression of naked DNA in human, pig, and mouse skin. *J Clin Invest* 97:2911–6

Irvine AD, McLean WHI (1999) Human keratin diseases: the increasing spectrum of disease and subtlety of the phenotype–genotype correlation. *Br J Dermatol* 140:815–28

Khavari PA, Rollman O, Vahlquist A (2002) Cutaneous gene transfer for skin and systemic diseases. *J Intern Med* 252:1–10

Lane EB (1993) Keratins. In: *Connective tissue and its heritable disorders molecular, genetic and medical aspects* (Royce P, Steinmann B, eds), New York: Wiley-Liss Inc, 237–47

Lane EB, Rugg EL, Navsaria H, Leigh IM, Heagerty AH, Ishida-Yamamoto A.,*et al.* (1992) A mutation in the conserved helix termination peptide of keratin 5 in hereditary skin blistering. *Nature* 356:244–6

Layzer JM, McCaffrey AP, Tanner AK, Huang Z, Kay MA, Sullenger BA (2004) *In vivo* activity of nuclease-resistant siRNAs. *RNA* 10:766–71

Leachman SA, Kaspar RL, Fleckman P, Florell SR, Smith FJD, McLean WHI *et al.* (2005) Clinical and pathological features of pachyonychia congenita. *J Investig Dermatol Symp Proc* 10:3–17

Lewin AS, Glazer PM, Milstone LM (2005) Gene therapy for autosomal dominant disorders of keratin. *J Investig Dermatol Symp Proc* 10:47–61

Lin MT, Levy ML, Bowden PE, Magro C, Baden L, Baden HP *et al.* (1999) Identification of sporadic mutations in the helix initiation motif of keratin 6 in two pachyonychia congenita patients: further evidence for a mutational hot spot. *Exp Dermatol* 8:115–9

McCaffrey AP, Nakai H, Pandey K, Huang Z, Salazar FH, Xu H *et al.* (2003) Inhibition of hepatitis B virus in mice by RNA interference. *Nat Biotechnol* 21:639–44

McLean WHI, Rugg EL, Lunny DP, Morley SM, Lane EB, Swensson O *et al.* (1995) Keratin 16 and keratin 17 mutations cause pachyonychia congenita. *Nat Genet* 9:273–8

McLean WHI, Smith FJD, Cassidy AJ (2005) Insights into genotype–phenotype correlation in pachyonychia congenita from the human intermediate filament mutation database. *J Investig Dermatol Symp Proc* 10:31–6

Miller VM, Xia H, Marrs GL, Gouvion CM, Lee G, Davidson BL *et al.* (2003) Allele-specific silencing of dominant disease genes. *Proc Natl Acad Sci USA* 100:7195–200

Morrissey DV, Blanchard K, Shaw L, Jensen K, Lockridge JA, Dickinson B *et al.* (2005) Activity of stabilized short interfering RNA in a mouse model of hepatitis B virus replication. *Hepatology* 41:1349–56

Omary MB, Coulombe PA, McLean WH (2004) Intermediate filament proteins and their associated diseases. *N Engl J Med* 351:2087–100

Pines M, Domb A, Ohana M, Inbar J, Genina O, Alexiev R *et al.* (2001) Reduction in dermal fibrosis in the tight-skin (Tsk) mouse after local application of halofuginone. *Biochem Pharmacol* 62:1221–7

Prud'homme GJ, Glinka Y, Khan AS, Draghia-Akli R (2006) Electroporation-enhanced nonviral gene transfer for the prevention or treatment of immunological, endocrine and neoplastic diseases. *Curr Gene Ther* 6:243–73

Sawamura D, Akiyama M, Shimizu H (2002) Direct injection of naked DNA and cytokine transgene expression: implications for keratinocyte gene therapy. *Clin Exp Dermatol* 27:480–4

Schwarz DS, Ding H, Kennington L, Moore JT, Schelter J, Burchard J *et al.* (2006) Designing siRNA that distinguish between genes that differ by a single nucleotide. *PLoS Genet* 2:e140

Shaner NC, Campbell RE, Steinbach PA, Giepmans BN, Palmer AE, Tsien RY (2004) Improved monomeric red, orange and yellow fluorescent proteins derived from *Discosoma* sp. red fluorescent protein. *Nat Biotechnol* 22:1567–72

Shaner NC, Steinbach PA, Tsien RY (2005) A guide to choosing fluorescent proteins. *Nat Methods* 2:905–9

Smith F (2003) The molecular genetics of keratin disorders. *Am J Clin Dermatol* 4:347–64

Smith FJD, Kaspar RL, Schwartz ME, McLean WHI, Leachman SA (2006) Pachyonychia congenita. *GeneReviews*; www.genetests.org/profiles/pc

Smith FJD, Liao H, Cassidy AJ, Stewart A, Hamill KJ, Wood P *et al.* (2005) The genetic basis of pachyonychia congenita. *J Investig Dermatol Symp Proc* 10:21–30

Smith FJD, McKenna KE, Irvine AD, Bingham EA, Coleman CM, Uitto J *et al.* (1999) A mutation detection strategy for the human keratin 6A gene and novel missense mutations in two cases of pachyonychia congenita type 1. *Exp Dermatol* 8:109–14

Song E, Lee SK, Wang J, Ince N, Ouyang N, Min J *et al.* (2003) RNA interference targeting Fas protects mice from fulminant hepatitis. *Nat Med* 9:347–51

Soutschek J, Akinc A, Bramlage B, Charisse K, Constien R, Donoghue M *et al.* (2004) Therapeutic silencing of an endogenous gene by systemic administration of modified siRNAs. *Nature* 432:173–8

Steinert PM, Yang JM, Bale SJ, Compton JG (1993) Concurrence between the molecular overlap regions in keratin intermediate filaments and the locations of keratin mutations in genodermatoses. *Biochem Biophyl Res Commun* 197:840–8

Wang Q, Contag CH, Ilves H, Johnston BH, Kaspar RL (2005) Small hairpin RNAs efficiently inhibit hepatitis C IRES-mediated gene expression in human tissue culture cells and a mouse model. *Mol Ther* 12: 562–8

Wang Q, Ilves H, Chu P, Contag CH, Leake D, Johnston BH *et al.* (2007) Delivery and inhibition of reporter genes by small interfering RNAs in a mouse skin model. *J Invest Dermatol* doi:10.1038/sj.jid.5700891

Wesche-Soldato DE, Chung CS, Lomas-Neira J, Doughty LA, Gregory SH, Ayala A (2005) *In vivo* delivery of caspase-8 or Fas siRNA improves the survival of septic mice. *Blood* 106:2295–301

Woll S, Windoffer R, Leube RE (2005) Dissection of keratin dynamics: different contributions of the actin and microtubule systems. *Eur J Cell Biol* 84:311–28

Wong P, Domergue R, Coulombe PA (2005) Overcoming functional redundancy to elicit pachyonychia congenita-like nail lesions in transgenic mice. *Mol Cell Biol* 25:197–205